Interferometric out-of-focus imaging of irregular rough particles: from the estimation of their sizes to the determination of morphological properties

Marc Brunel[1,*], Sara Gonzalez Ruiz[2], Justin Jacquot[1,3], Lila Ouldarbi[1], Sébastien Coëtmellec[1], Gérard Gréhan[1], Jeroen van Beeck[2]

[1]UMR 6614 CORIA, Normandie Université, CNRS, Université et INSA de Rouen, Saint-Etienne du Rouvray, France
[2]Von Karman Institute for Fluid Dynamics, Rhode-Saint-Genèse, Belgium
[3]Zodiac Aerospace, 1 rue Pierre Curie - B.P. 1 -78373 Plaisir Cedex - FRANCE
*corresponding author: marc.brunel@coria.fr

Abstract We present a mathematical formalism to predict the speckle-like out-of-focus patterns created by irregular particles present in an air flow, when they are illuminated by a laser sheet. We show that it is not necessary to describe rigorously the scattering properties of the irregular objects to predict some physical properties of their interferometric out-of-focus patterns. The objects are described by an ensemble of Dirac emitters.. The size of the central peak of the 2-dimensional autocorrelation of the pattern allows the prediction of the size of the scattering element. The method can be applied to particles in a size range from a tenth of micrometers to the millimeter. We discuss the conditions under which the speckle patterns are representative of the particle size, and the configurations where the speckle pattern is only linked to the aperture itself and to the defocus parameter. We show that the 2-dimensional Fourier transform of the speckle-like out-of-focus image of an irregular rough particle is given by the 2 dimensional-autocorrelation of the shape of the particle. Using a matrix transfer based-formulation, we further determine the exact scaling factors between both functions, whatever the imaging system is. The method is tested in a cooling chamber to measure the size of frozen droplets. Liquid droplets fall in the column, freeze and are transformed in irregular ice particles. Interferometric out-of-focus images are then recorded (through optical windows) and the characteristics of the ice particles are analyzed from the study of the speckle-like out-of-focus patterns.
Keywords: Light scattering, Irregular particles, interferometric particle imaging

1 Introduction

The development of techniques that can characterize irregular particles is essential because they are commonly present in our environment: coal, sand, ashes, ice crystals… Optical techniques are particularly interesting because the wavelength of visible light is well adapted to the micronic dimensions of many particles. Most simple optical technique is a direct visualization using conventional imaging. Many interferometric techniques can be further used: they are based on the interpretation of the light scattering properties of the particles. Some of them are particularly famous for droplet characterization as rainbow refractometry [1], interferometric out-of-focus imaging [2,3], digital holography [4-7]. Nevertheless, the use of most of them remains an important challenge for the characterization of irregular particles. There is indeed no theoretical model that can describe the light scattering properties of any irregularly-shaped particle [8]. It is necessary to make some assumptions about the light scattering process if we want to predict statistically some parameters of the interferometric patterns generated by the particles. Then characterization methods can be developed.
We work on the development of an airborne instrument to characterize droplets in the atmosphere [9]. It is based on interferometric out-of-focus imaging [3,10-15]. This technique can indeed use real-time algorithms to deliver histograms of the sizes of droplets from a sole image [16]. The possible extension to the characterization of ashes or ice crystals would be particularly interesting. Unfortunately, it is first important to understand which kind of image can be observed, whether this image contains an information about the size of the particles, and whether it can be analyzed simply to deliver histograms of sizes of irregular particles. This is the aim of this paper. We will describe the work that we have developed in order to answer these questions. Using simplified assumptions, we will show that we can predict some properties of the out-of-focus images of irregular rough particles. These characteristics will then be used to evaluate the size and some informations about the morphology of the particles.

2 Simplified theory of the light scattering by irregular rough particles

There is no general theory that can describe the scattering properties of any arbitrarily-shaped rough particle when it is illuminated by a laser beam. Nevertheless, simplifications can be done which allow to obtain some quantitative informations on the particle from a scattering pattern. Figure 1 (left) shows the shadographic image of a sand particle. Figure 1 (right) shows the image of the same particle when it is illuminated by a HeNe laser beam. In this case, the sand particle appears as if it was composed of a high number of emitting spots located all over the global shape of the particle [17-20]. From this observation, we assume that the electric field emitted by an irregular rough particle can be written [18,19]:

$$G_0(x_0,y_0) = \sum_{j=1}^{N_{gp}} \alpha_j \; e^{i\,\varphi_j} \; \delta\big(x_0 - a_j, y_0 - b_j\big) \tag{1}$$

where the δ functions are Dirac functions. a_j and b_j are the transverse coordinates of glare point denoted j. N_{gp} is the number of point emitters to be considered. They are located over the global shape of the particle. z represents the optical longitudinal axis of the imaging set-up. We assume that all glare points are located in the plane z=0. x_0 and y_0 denote the transverse axes in the plane of the particle.

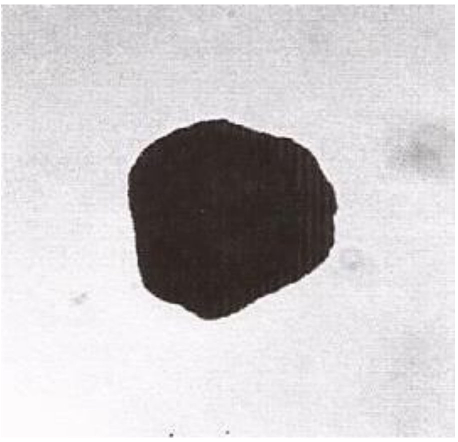
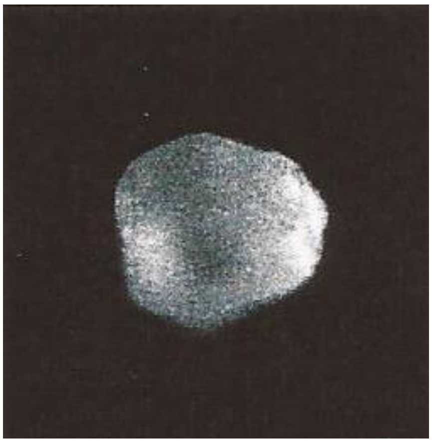

Fig. 1 Shadowgraphic image of a sand particle (left), image of the same sand particle when it is illuminated by a HeNe laser beam (right).

According to references [18-20], and neglecting the role of the aperture of the imaging system (big aperture), the electric field can be evaluated in the plane of the CCD sensor from a generalized Huygens Fresnel integral. We obtain the following expression of the electric field in the plane of the CCD sensor :

$$G(x,y,z) = \sum_{j=1}^{N_{gp}} \frac{\alpha_j}{i\,\lambda\,B} \; e^{i(\theta_j+\varphi_j)} e^{i\left(\frac{2\pi}{\lambda}\,\Delta(z)\right)} \tag{2}$$

where z is the longitudinal position of the CCD sensor, x and y are the transverse coordinates in the plane of the CCD sensor.

$$\theta_j = \frac{\pi}{\lambda B}\left[A\big(a_j^2 + b_j^2\big) - 2\big(a_j\,x + b_j\,y\big) + D(x^2+y^2)\right] \tag{3}$$

The different A, B, C and D parameters are the coefficients of the optical transfer matrix between the plane of the different emitters and the plane where the aperture is located. $\Delta(z)$ is the optical path between these two planes. The expression of the intensity in the plane of the CCD sensor is given by: $I(x,y,z) \propto G(x,y,z).\,G(x,y,z)^*$. We can then define $TF_{2D}[I(x,y)](u,v)$ the 2 dimensional Fourier transform of the intensity $I(x,y,z)$ and $A_{2D}[G_0(x_0,y_0)]\big(\Delta_x,\Delta_y\big)$ the 2-dimensional autocorrelation function of the initial electric field (i.e. the repartition of the emitters on the scattering object). According to relations (1), (2) and (3), we can demonstrate that [20]:

$$|TF_{2D}[I](\lambda\, B\, u, \lambda\, B\, v)| \propto \left|A_{2D}[G_0]\left(\Delta_x, \Delta_y\right)\right| \qquad (4)$$

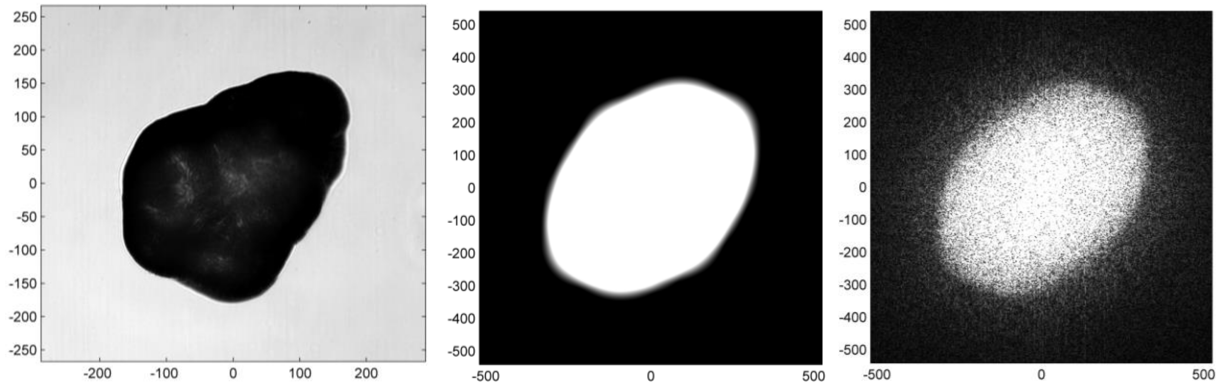

Fig. 2 Shadowgraphic image of a sand particle (left), 2D-autorrelation of the binarized shape of the particle (middle), 2D-Fourier transform of the experimental interferometric out-of-focus image of this particle (right).

Figure 2 illustrates this relation. It shows first the shadowgraphic image of a sand particle (left), the 2D-autorrelation of the binarized shape of the particle (middle) and the 2D-Fourier transform of the experimental interferometric out-of-focus image of this particle (right). The parameters and scaling factors are those of the experiment and satisfy relation (4). Other sand particles were tested. In all cases, the relation (4) is satisfied, and the scaling factors match well [20].
In a second step, it is possible to simulate the influence of the exact aperture of the set-up. It can be done using a simple description of the aperture, using geometrical optics [21], an exact description of the aperture using an expansion of the Airy function over the basis of Bessel functions [21], or an approached expression using the expansion of the aperture over a basis a Gaussian functions [18,19].

3 Simplified analysis for the determination of the size of irregular rough particles from their speckle-like interferometric out-of-focus image

Qualitatively, the main information (contained in relation (4)) is that the speck of light of the speckle-like out of-focus image of an irregular rough particle is inversely proportional to the size of the particle. Figure 3 illustrates this. It shows the interferometric out-of-focus images of rough particles described by an ensemble of 40 emitting spots randomly located over an half-sphere of radius 20 µm (left), 40 µm (middle) and 80 µm (right).

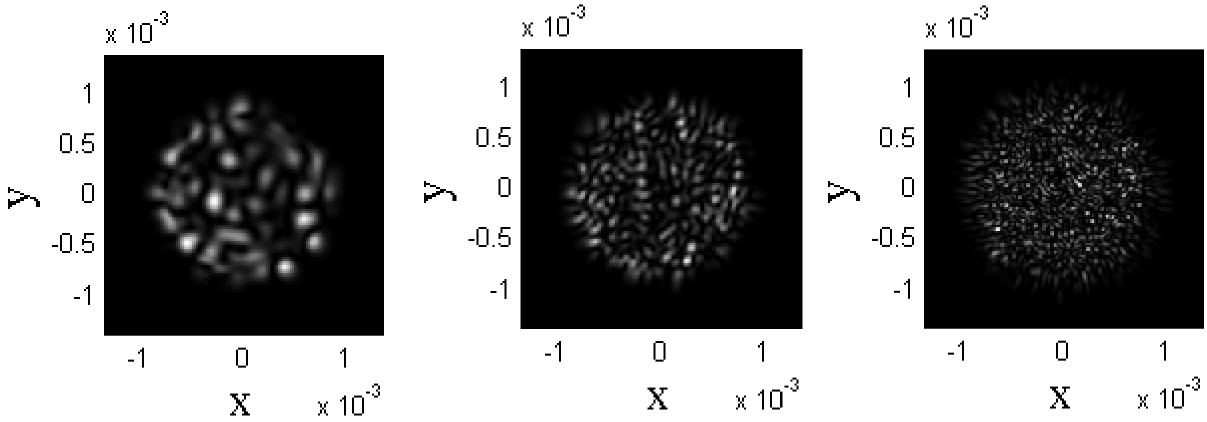

Fig. 3 Three simulated out-of-focus images of spherical particles: the particles are assimilated to an ensemble of 50 Dirac emitters randomly located over an half-sphere of radius 20 µm (left), 40 µm (middle) and 80 µm (right).

In a speckle pattern, the size of the speck of light can be defined through the 2D-autocorrelation of the pattern [22]. The 2D-autocorrelations of the three patterns presented in figure 3 are shown in figure 4. In all cases, we observe an intense central peak whose size gives the statistical dimension of the speck of light. This central peak is centered on a much larger 2D-pedestal. These curves confirm the inverse relation which links size of particle and size of the speck of light in the speckle-like patterns.

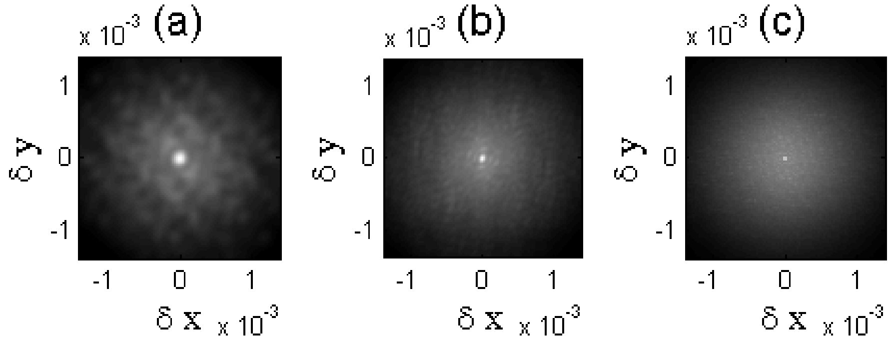

Fig. 4 2D-Autocorrelations of the interferometric out-of-focus patterns of figures 3. All axes are expressed in meters.

Quantitatively, the distance Δ between the two farthest emitters describing the irregular particle is approximately given by [19]:

$$\Delta = \alpha\lambda B/\delta_{speck} \tag{5}$$

where δ_{speck} is the width of the central peak of the 2D-autocorrelation (the width is evaluated between the two points at 70% of the peak's maximum), B is the B-coefficient of the optical transfer matrix describing the imaging system from the particle to the plane of the CCD sensor, λ is the wavelength of the illuminating laser, and α is a correction factor due to autocorrelation operation (around 0.9). Note that this procedure can be extended to a 2D-analysis, considering an elliptic repartition of the emitters when the particle is not circular but has an ellipsoidal shape. We determine then the orientation of the big- and small- axes of the central peak of the 2D-autocorrelation of the speckle-pattern. We then deduce the size of the particle along these two axes using relation (5) separately for both axes [19,20].
As an example, figure 5(a) shows the experimental interferometric out-of-focus image of a NaCl salt crystal. Using previously described procedure, we evaluate the size and the ellipticity of the speck of light, and then the size and ellipticity of an equivalent particle represented by 80 punctual emitters located over an half-ellipsoid of dimensions 600x400 micrometers. The simulated out-of-focus pattern is presented in figure 5(b). Its speck of light has same size and ellipticity (statistically).

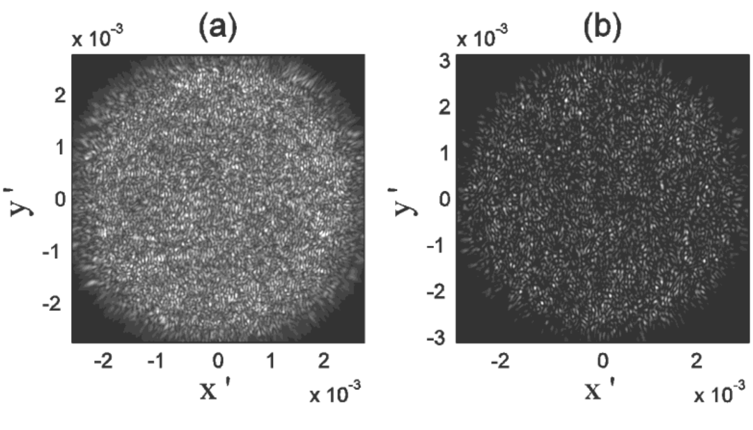

Fig. 5 Experimental out-of-focus image of a NaCl salt particle (a) and simulated out-of-focus image of an ensemble of 80 Dirac emitters randomly distributed on a half-ellipsoid of dimensions 600x400 micrometers (b). Axes in meters.

It must be noted that the aperture of the imaging system plays an important role in the limits of the method: when the size of the particle is so big that the out-of-focus images of the farthest spots do not interfere anymore, the speckle pattern that is observed is no more representative of the size of the particle but on the set of parameters : aperture, defocus parameter Δp. In the case represented in figure 6, this limit size of the particle is represented by parameter X_{max}.

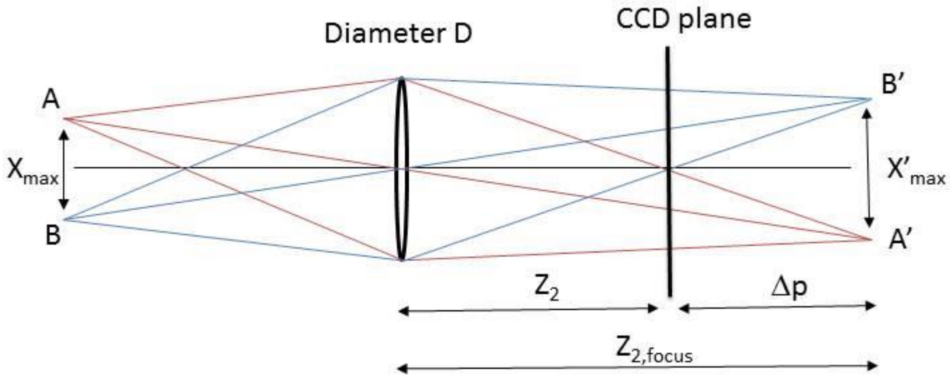

Fig. 6 Size limit of the irregular rough particles to be measured using interferometric out-of-focus imaging.

4 Analysis of the interferometric out-of-focus images of frozen droplets

In previous studies, this formalism has been applied to the experimental characterization of NaCl salt crystals or sand particles. Let us now see if this formalism can be applied to the characterization of ice particles. In order to analyze frozen droplets, we have realized a cold chamber as done by Barkey and coworkers [23]. It consists of an refrigerated cylindrical column (750 mm tall, 110 mm large). Water droplets from a MD-K 140 728 Microdrop generator (approximately 100 µm diameter) fall from the top of the column and are cooled. Three BK7 windows are positioned at the bottom of the chamber. They allow optical measurement of light scattering by liquid and frozen droplets. The global set-up is presented in figure 7.
First, 4 ns, 532 nm pulses (from a frequency-doubled Nd:YAG laser) are sent into the cold chamber. The beam is collimated in order to obtain a plane wave illumination inside the column. The field scattered by the inside-particles is observed around the scattering angle θ=90°. It is imaged through the window with a lens (focus length f) on a CCD sensor. The CCD sensor operates in an out-of-focus plane. The out-of-focus images are recorded with a 2048x2048 camera and the pixel's size is 5.5 µm.
A digital in-line holography set-up is added: the light source is a CW HeNe laser diode emitting at the wavelength 632.8 nm. Holograms are recorded with a second camera (similar to the first one). We use an in-line configuration, which means that the CCD sensor is located after the particles and the output window in the direction of the He-Ne laser beam. Numerical reconstruction of the holograms is performed using a classical Fresnel transform. Both cameras are synchronized temporally. They both consider the same volume in the column. It means that the same column can be viewed from out-of-focus imaging at 90° scattering angle, and from hologram reconstruction in the forward direction.
Figure 8 shows the reconstruction of the digital hologram of a frozen droplet while figure 9 shows the corresponding interferometric out-of-focus image of the same particle. From the reconstructed hologram, we deduce that the size of the frozen droplet is $120 \pm 10\mu m$ along the vertical axis. From the out-of-focus image, we evaluate the 2D-autocorrelation of the speckle-like pattern. We present then in figure 9 (right) the zoom of the central peak of this 2D-autocorrelation function. From the size of the central peak, we can deduce the size of the frozen droplet along the vertical axis, respecting the method described in previous section. We obtain is $125 \pm 15\mu m$. Both values obtained using digital holography and out-of-focus imaging are near. The evaluation using interferometric particle imaging (IPI) appears thus to be correct for frozen

droplets.
This result is an important point which indicates that the size of frozen droplets could be evaluated using IPI with a relatively good accuracy. Nevertheless further tests are needed. In our case, frozen droplets are more or less fine hail and not ice crystals. Our procedure is well adapted to rough objects that can be represented by a wide number of punctual emitters located all over the shape of the particle. In the case of transparent crystals, it could be different : lower number of emitting spots, parts of the global shape where no emitting spots are present… In the future, it is first important to establish the accuracy on a wide number of out-of-focus images of frozen droplets, and to evaluate the rate of errors. Future studies should then be focused on the possibility to extend the analysis to a wide range of ice crystal morphologies. It will require important work in order to realize experimentally different families of ice crystals that are observable in the atmosphere, and to realize the characterizations on a high number of crystals.

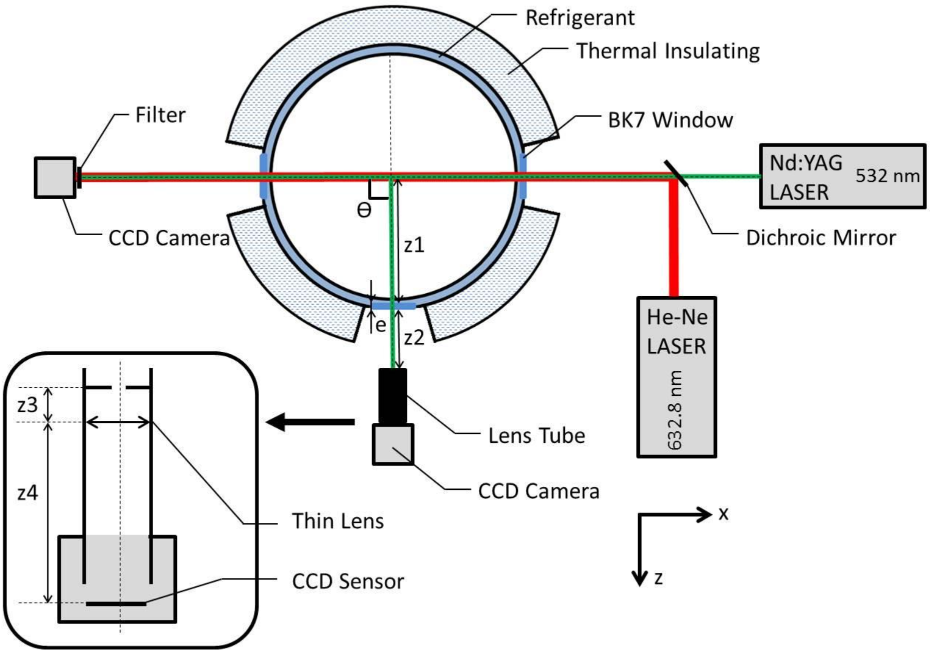

Fig. 7 Experimental set-up to record simultaneously digital holograms and out-of-focus images of frozen droplets.

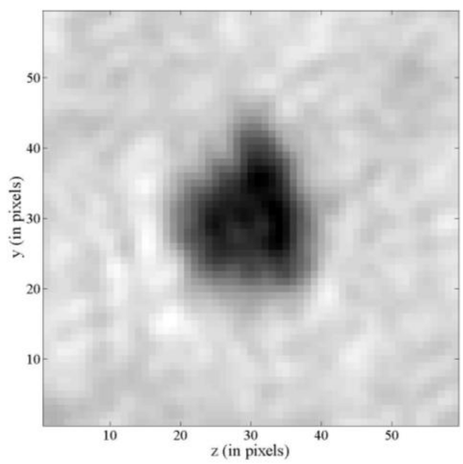

Fig. 8 Reconstructed frozen droplet from a digital in-line hologram (5.5 microns per pixel).

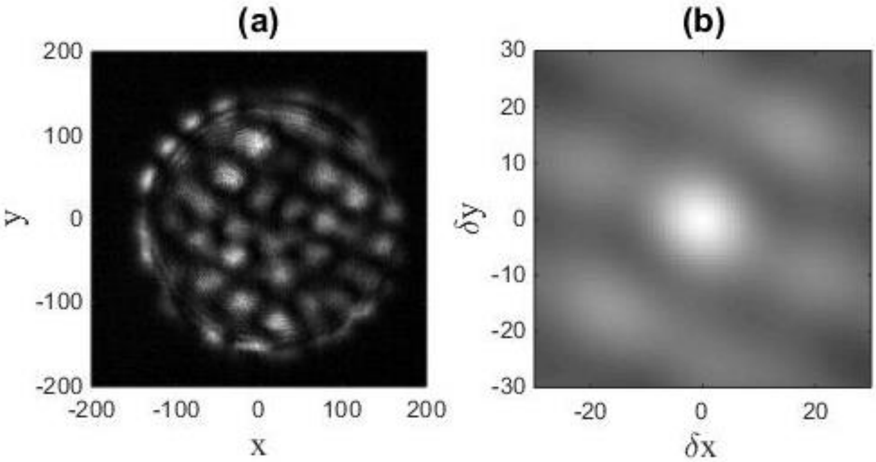

Fig. 9 Interferometric out-of-focus image of the frozen droplet (a) and zoom of the central peak of the 2D-autocorrelation of this pattern. All axes are expressed in pixels (5.5 microns per pixel).

5 Extreme events: intense peaks

Considering the development of commercial instruments, it is essential that the CCD sensor can support without damage the scattered intensity, for a wide range of particle's sizes and forms. In the case of irregular rough particles which give speckle-like out-of-focus images, it is thus important to predict the conditions where a particle can generate very intense specks of light. It is indeed established that linear systems can exhibits rogue wave statistics in the transverse spatial plane, for example the case of speckle pattern observed at the output of a strongly multimode fiber [24]. We do not plan to realize a fundamental study about the possibility of observing rogue patterns in our case. Nevertheless, we will try to predict the possibility to observe extreme events that could damage our sensor.

In order to do this, we have first considered a rough object which can be assimilated to an ensemble of N_{gp} punctual emitters. An example of repartition of these glare points is presented in figure 10. The emitters are located in a square whose dimensions are $50\ \mu m \times 50\mu m$. The amplitude of all emitters is the same. Figure 11 (on the left) shows a typical out-of-focus image obtained when the phase of all emitters is a random variable in the range $[0,2\pi]$. This assumption is indeed the most probable in our case: we are interested in the characterization of particles in the size domain from a tenth of micrometers to hundreds of micrometers. For spherical droplets, the phase shift introduced between the two glare points (which represent the reflected beam and the beam refracted by the droplet without any internal reflection) is then much higher than 2π. In the case of irregular particles, it is assumed that the phase φ_i of each emitter is a random variable in the range $[0,2\pi]$. For comparison, figure 11 (on the right) shows now a typical out-of-focus image obtained when the phase of all emitters is a random variable in the range $[0,\pi]$. In this case, we observe an intense central speck of light whose intensity is three times higher than the most intense peak of the speckle-pattern presented on the left of the same figure.

We have then calculated 11000 out-of-focus patterns, for 11000 random repartitions of the 50 emitters. In all cases, the amplitude of each emitter is a random value in the interval [0,1], and its phase is a random value in the range $[0, 2\pi]$. Depending on the relative positions, amplitudes and phases of the emitters, the maximal intensity measured in the image can vary in a proportion of approximately 1 to 10. The results are presented in figure 12. The CCD sensor should thus be able to measure variations of intensities in a ratio 1 to 10, for the same size of irregular particles.

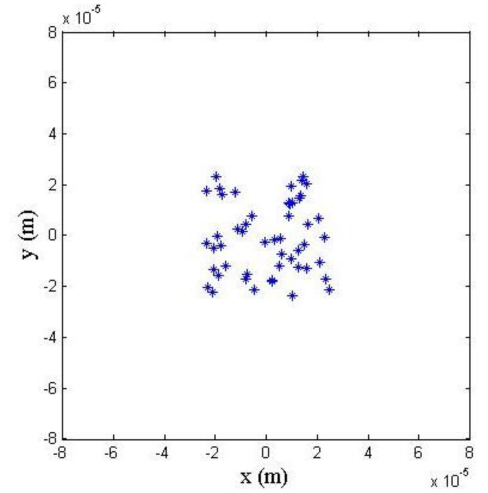

Fig. 10 Repartition of 50 punctual emitters

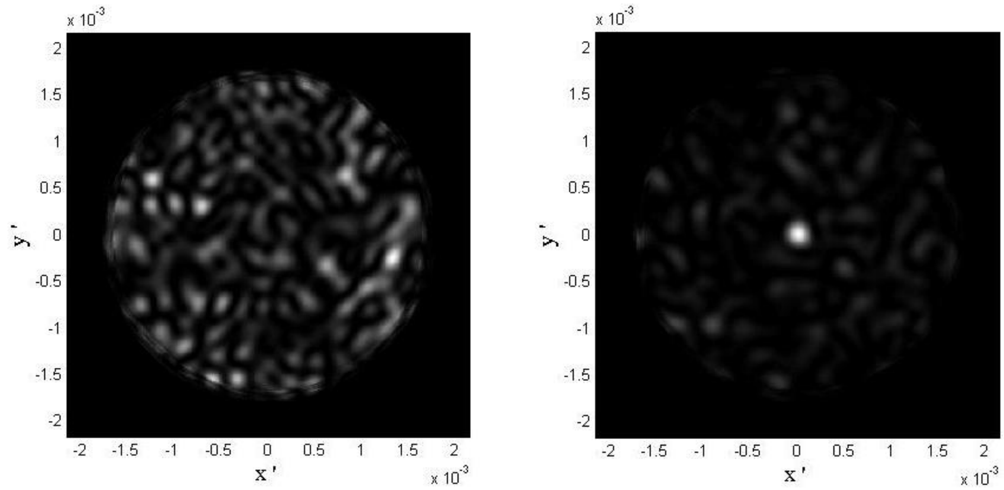

Fig. 11 Speckle-like pattern predicted when the phase of the 50 emitters is a random value in the range $[0,2\pi]$ (left), and in the range $[0,\pi]$ (right). Axes in meters.

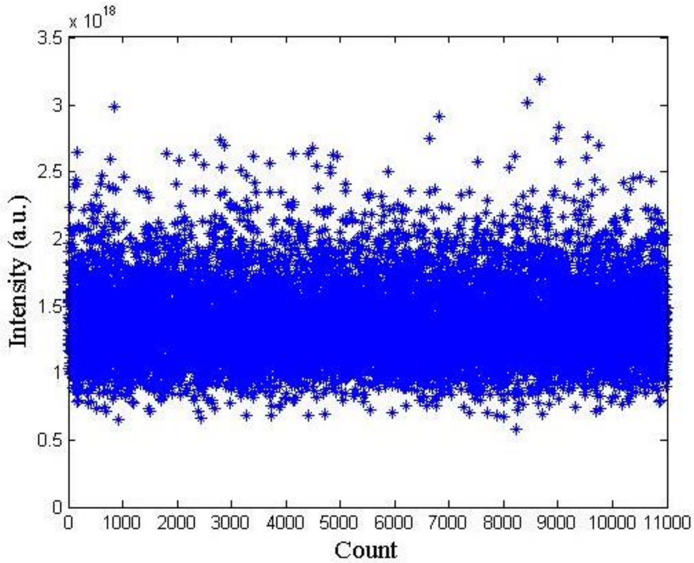

Fig. 12 Maximum intensity recorded for 11000 interferometric out-of-focus images of particles represented by 50 punctual emitters located in a square whose dimensions are $50\ \mu m \times 50\mu m$.

6 Conclusion

We have developed a mathematical formalism to predict the speckle-like out-of-focus patterns created by irregular rough particles present in an air flow, when they are illuminated by a laser sheet. It is not necessary to describe rigorously the scattering properties of the irregular objects to predict some physical properties of their interferometric out-of-focus patterns. The objects are described by an ensemble of Dirac emitters.. The size of the central peak of the 2-dimensional autocorrelation of the pattern allows the prediction of the size of the scattering element. The 2-dimensional Fourier transform of the speckle-like out-of-focus image of an irregular rough particle is given by the 2 dimensional-autocorrelation of the shape of the particle. Using a matrix transfer based-formulation, the exact scaling factors between both functions can be determined whatever the imaging system is. The method is tested with frozen droplets. Interferometric out-of-focus images are recorded. The size of the ice particles is then evaluated using our methods and compared to the size obtained simultaneously using digital holography. These first results offer relatively good quantitative agreement. However, important future work has to be done in order to evaluate statistically the accuracy and the error rate of the procedure with a wide number of particles, for different morphologies and different natures of the irregular particles under test (ashes, crystals…).

Acknowledgments

The authors thank the French National Agency through the program Investissements d'Avenir (ANR-10-LABX-09-01) LabEx EMC[3]. These results have further received funding from the European Union Seventh Framework Programme (FP7/2007-2013): project EUFAR (EUropean Facility for Airborne Research), and project HAIC (High Altitude Ice Crystal) under grant agreement n°ACP2-GA-2012-314314.

References

[1] Nussenzveig H M (1977) The theory of the rainbow. Scientific American pp 116-128

[2] Glantschnig W J, Chen S H (1981) Light scattering from water droplets in the geometrical optics approximation, Applied Optics, vol. 20, pp 2499-2509. doi: http://dx.doi.org/10.1364/AO.20.002499

[3] Glover A R, Skippon S M, Boyle R D (1995) Interferometric laser imaging for droplet sizing: a method for droplet-size measurement in sparse spray systems. *Applied Optics*, vol. 34, pp 8409–8421. doi: http://dx.doi.org/10.1364/AO.34.008409

[4] Schnars U, Jüptner W P (1994) Direct recording of holograms by a CCD target and numerical reconstruction, *Applied Optics*, vol. 33, pp 179-181. doi: http://dx.doi.org/10.1364/AO.33.000179

[5] Katz J, Sheng J (2010) Applications of Holography in Fluid Mechanics and Particle Dynamics, *Annual Review of Fluid Mechanics,* vol. 42, pp 531-555. doi: 10.1146/annurev-fluid-121108-145508

[6] Buraga-Lefebvre C, Coetmellec S, Lebrun D, Ozkul C (2000) Application of wavelet transform to hologram analysis: three-dimensional location of particles, *Optics and Lasers in Engineering*, vol. 33, pp 409-421. doi:10.1016/S0143-8166(00)00050-6

[7] Brunel M, Wichitwong W, Coetmellec S, Masselot A, Lebrun D, Gréhan G, Edouard G (2015) Numerical models for exact description of in-situ digital in-line holography experiments with irregularly-shaped arbitrarily-located particles, *Applied Sciences,* vol. 5, pp 62-76. doi:10.3390/app5020062

[8] Van de Hulst H C (1981) Light Scattering by Small Particles, General publishing company.

[9] Porcheron E, Lemaitre P, Van Beeck J, Vetrano R, Cuvelier P, Brunel M, Gréhan G, Guiraud L (2014) Development of the ALIDS spectrometer for airborne measurement of the droplets size in clouds. Proceeding of the 16th International Symposium on Flow Visualization. June 24-28, 2014, Okinawa, Paper 1296.

[10] Mounaïm-Rousselle C, Pajot O (1999) Droplet Sizing by Mie Scattering Interferometry in a Spark

Ignition Engine, *Particle and Particle System Characterization*, vol. 16, pp 160-168.

[11] Kawaguchi T, Akasaka Y, Maeda M (2002) Size measurements of droplets and bubbles by advanced interferometric laser imaging technique, *Measurement Science and Technology*, vol. 13, pp 308-316. doi: 10.1088/0957-0233/13/3/312

[12] Damaschke N, Nobach H, Tropea C (2002) Optical limits of particle concentration for multi-dimensional particle sizing techniques in fluid mechanics, *Experiments in Fluids*, vol. 32, pp 143-152. doi: 10.1007/s00348-001-0371-x

[13] Albrecht H E, Borys M, Damaschke N, Tropea C (2003) Laser Doppler and Phase Doppler measurement techniques, Springer Verlag, Berlin.

[14] Dehaek S, Van Beck J P A P (2007) Designing a maximum precision interferometric particle imaging set-up, *Experiments in Fluids*, vol. 42, pp 767-781. doi: 10.1007/s00348-007-0286-2

[15] Shen H, Coetmellec S, Grehan G, Brunel M (2012) ILIDS revisited: elaboration of transfer matrix models for the description of complete systems, *Applied Optics,* vol. 51, pp 5357-5368. doi: http://dx.doi.org/10.1364/AO.51.005357

[16] Quérel A, Lemaitre P, Brunel M, Porcheron E, Gréhan G (2010) Real-time global interferometric laser imaging for the droplet sizing (ILIDS) algorithm for airborne research, *Measurement Science and Technology,* vol. 21. 015306. doi:10.1088/0957-0233/21/1/015306

[17] Ulanowski Z, Kaye P H, Hirst E, Greenaway R S, Cotton R J, Hesse E, Collier C T (2014) Incidence of rough and irregular atmospheric ice particles from Small Ice Detector 3 measurements, *Atmospheric Chemical Physics*, vol. 14, pp 1649-1662. doi:10.5194/acp-14-1649-2014

[18] Brunel M, Shen H, Coëtmellec S, Gréhan G, Delobel T (2014) Determination of the size of irregular particles using interferometric out-of-focus imaging. *International Journal of Optics*, Article ID 143904. doi: http://dx.doi.org/10.1155/2014/143904

[19] Brunel M, Coetmellec S, Gréhan G, Shen H (2014) Interferometric out-of-focus imaging simulator for irregular rough particles. *Journal of the European Optical Society: Rapid Publications*, vol. 9, 14008. doi: http://dx.doi.org/10.2971/jeos.2014.14008

[20] Brunel M, Gonzalez Ruiz S, Jacquot J, van Beeck J (2015) On the morphology of irregular rough particles from the analysis of speckle-like interferometric out-of-focus images. *Optics Communications*, vol. 338, pp 193-198. doi : http://dx.doi.org/10.1016/j.optcom.2014.10.053

[21] Brunel M, Ouldarbi L, Shen H, Gréhan G, Coëtmellec S (2015) Limits of rough particle's sizing with low out-of-focus interferometric imaging. To appear in *Particuology*. doi: http://dx.doi.org/10.1016 /j.partic.2014.07.008

[22] Goodman J W (2009) Speckle phenomena in optics. Theory and Applications, Roberts and Company Publishers.

[23] Barkey B, Bailey M, Liou F N, Hallet J (2002) Light-scattering properties of plate and column ice crystals generated in a laboratory cold chamber, *Applied Optics*, vol. 41, pp 5792 -5796. doi: http://dx.doi.org/10.1364/AO.41.005792

[24] Arecchi F T, Bortolozzo U, Montina A, Residori S (2011) Granularity and inhomogeneity are the joint generators of optical rogue waves. *Physical Review Letters, vol.* 106, 153901. doi: http://dx.doi.org/ 10.1103/PhysRevLett.106.153901